Supporting Information

Giorgio et al. 10.1073/pnas.1217823110

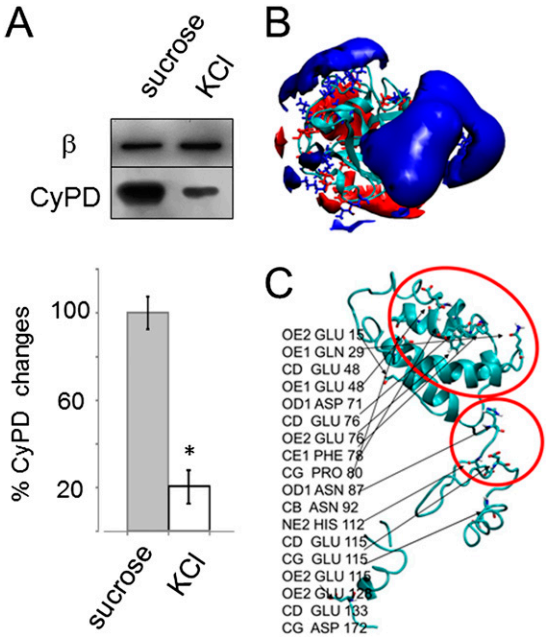

Fig. S1. Displacement of cyclophilin D (CyPD) from ATP synthase by KCl is consistent with electrostatic properties of CyPD-OSCP putative interaction sites. (*A*) Bovine heart mitochondria were suspended in sucrose (sucrose) or KCl buffer (KCl), treated with 1% (wt/vol) digitonin, and immunoprecipitated with anti-complex V antibody followed by SDS/PAGE. Immunodetection was performed with antibodies against β-subunit or CyPD as indicated. The ratio between CyPD and the corresponding β-subunit was measured (values are mean ± SE of three independent experiments). $*P = 0.0006$, Student *t* test. (*B*) CyPD electrostatic isopotential curves displayed in blue at 0.5 kT/(q mol) and red at −0.5 kT/(q mol). Secondary structure is represented with side chains displayed as blue (Arg and Lys) and red sticks (Asp and Glu). Cyclosporin A (CsA) binding site is shown. Oligomycin sensitivity-conferring protein (OSCP) isopotential curves are less smooth due to the size and complexity of the molecule in the context of ATP synthase. For this reason the lowest (i.e. most negative) average surface potential regions were considered instead as a putative binding region showing complementary electrostatic properties. (*C*) Side chain atoms (Protein Data Bank nomenclature) with the lowest average surface potential on OSCP. The two main regions of lowest surface potential are indicated by red ellipses.

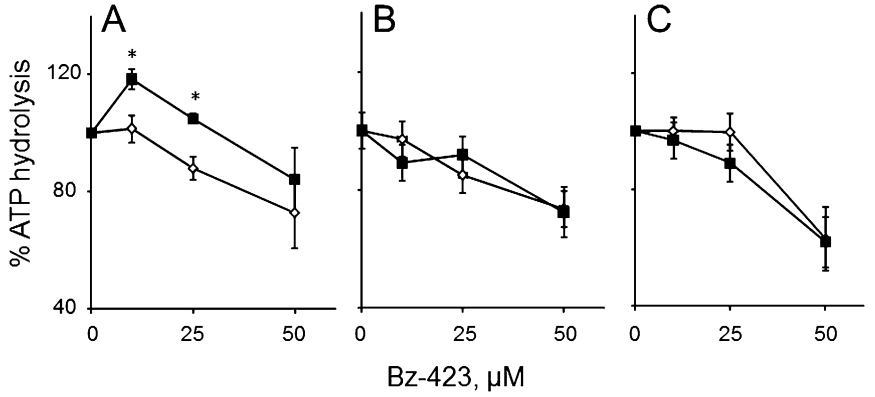

Fig. S2. CyPD affects the sensitivity of ATP synthase to inhibition by benzodiazepine 423 (Bz-423). Freshly prepared heart mitochondria from WT (*A* and *B*) and *Ppif*$^{-/-}$ mice (*C*) were treated for 10 min at room temperature with the indicated concentrations of Bz-423 in the presence of 1 (open symbols) or 10 mM (closed symbols) Pi, and the rate of oligomycin-sensitive ATP hydrolysis at 37 °C was measured after addition of 10 μM alamethicin. In *B*, 1.6 μM CsA was present. Data refer to triplicate samples ± SE of three independent experiments ($*P \leq 0.035$, Student *t* test). Absolute ATPase activity values (μmol/mg protein per minute) at 1 mM Pi were 3.51 ± 0.36, 3.35 ± 0.63, and 3.19 ± 0.33 for *A*, *B*, and *C*, respectively; absolute ATPase activity values (μmol/mg protein per minute) at 10 mM Pi were 2.88 ± 0.29, 3.25 ± 0.33, and 3.17 ± 0.26 for *A*, *B*, and *C*, respectively ($n = 3 \pm$ SE). Note that Pi only affects WT mitochondria in the absence of CsA, which we attribute to CyPD binding.

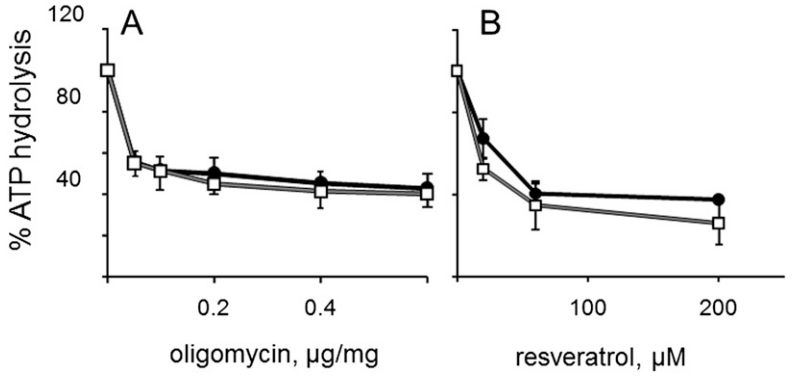

Fig. S3. Oligomycin and resveratrol inhibition of ATPase activity is not affected by CyPD. Freshly prepared mouse heart mitochondria from WT (closed symbols) and *Ppif* $^{-/-}$ mice (open symbols) were suspended in KCl buffer containing 10 mM Pi and treated for 10 min at room temperature in the presence of the indicated concentrations of (*A*) oligomycin or (*B*) resveratrol. The rate of oligomycin-sensitive ATP hydrolysis at 37 °C was measured after addition of 10 µM alamethicin. Reported values are average ± SE of three independent experiments.

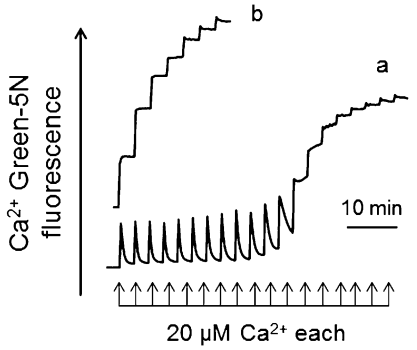

Fig. S4. ATP-driven Ca^{2+} uptake does not take place in the presence of oligomycin. The incubation medium contained no substrate, ATP, and an ATP-regenerating system and no further additions (trace a) or 1 µg/mL oligomycin (trace b). When indicated, Ca^{2+} was added (arrows).

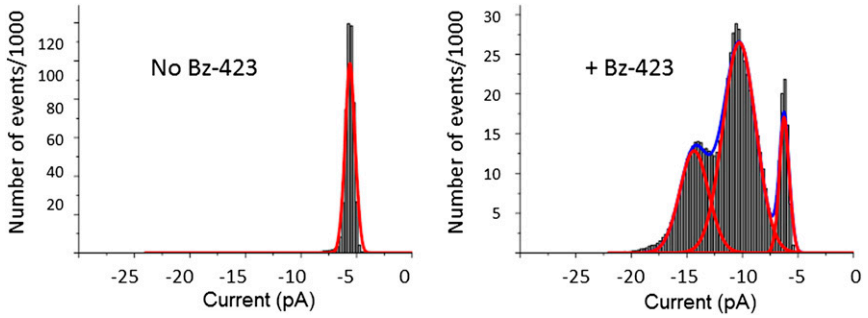

Fig. S5. Current amplitude histograms corresponding to the records exemplified in Fig. 5*A* in the text. Dimeric ATP synthase was used. Conditions: symmetrical 50 mM KCl, 1 mM Pi, and 0.3 mM Ca^{2+} without (*Left*) or with (*Right*) 0.1 mM Bz-423 in the *trans* compartment. V_{cis}: −60 mV. Sampling frequency: 10 KHz; 100-s segments of trace were binned in both cases.

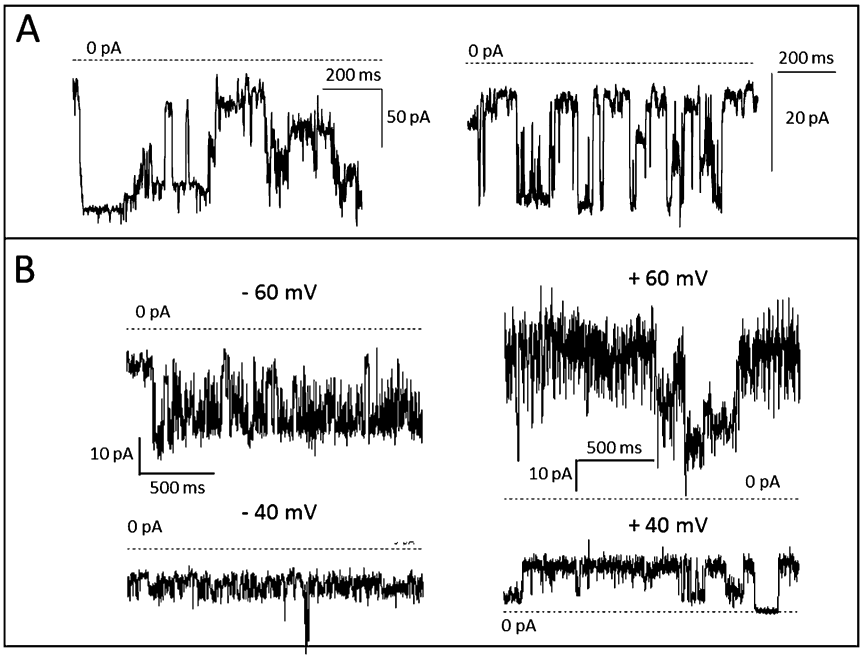

Fig. S6. Mitochondrial megachannel–permeability transition pore-like activity of reconstituted ATP synthase dimers. (*A*) Current records showing typical conductance levels at $V_{cis} = -140$ (*Left*) and −80 mV (*Right*) under the conditions of Fig. 5*C*. (*B*) Representative current traces recorded in 50 mM KCl, 1 mM Pi, and 3 mM Ca^{2+} added to the *trans* side at the indicated voltages are shown. Maximal conductance was 500 pS.

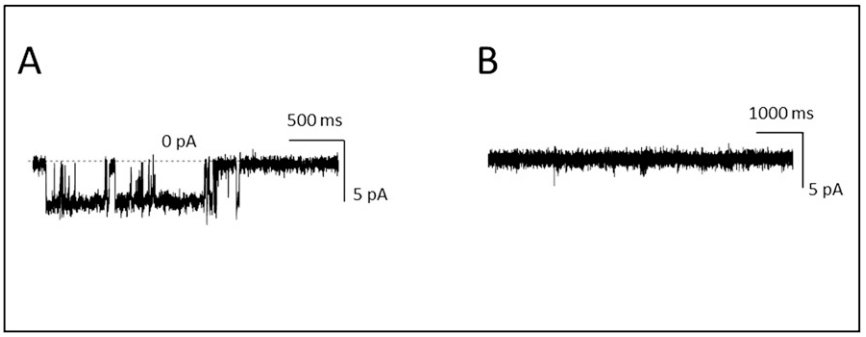

Fig. S7. Lack of mitochondrial megachannel-like activity with isolated complex I or dimeric ATP synthase after addition of atractyloside. (*A*) An illustration of channel activity observed after the addition of 0.1 mM atractyloside (*cis* side) to dimeric ATP synthase. Medium: 150 mM KCl, 0.3 mM Ca^{2+}, 1 mM Pi; $V_{cis} = -100$ mV. Channel conductance is 37 pS. (*B*) Representative current trace recorded at $V_{cis} = -60$ mV showing lack of activity after the addition of gel-purified complex I. Ionic conditions are the same as in Fig. S6*B*, except that KCl was 150 mM and 50 μM phenylarsine oxide was present in the *cis* compartment.

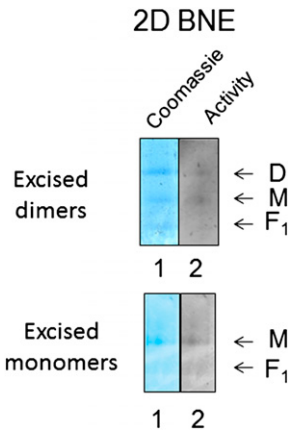

Fig. S8. Gel-purified ATP synthase dimers and monomers maintain enzymatic activity. Dimers (*Upper*) and monomers (*Lower*) were excised from the first blue native electrophoresis (BNE) gels (Fig. 4*A*), and they were eluted and resubjected to BNE and Coomassie blue (lane 1) and activity staining (lane 2).